Jinst

PUBLISHED BY IOP PUBLISHING FOR SISSA MEDIALAB

RECEIVED: *January 28, 2020*
REVISED: *February 6, 2020*
ACCEPTED: *March 10, 2020*
PUBLISHED: *April 6, 2020*

Imaging of bremsstrahlung X-rays from tritium water in a plastic bag using a LaGPS radiation imaging system

S. Yamamoto,[a,1] K. Nakanishi,[a] T. Furukawa,[a] H. Tomita,[b] K. Kamada[c] and A. Yoshikawa[c]

[a] *Radiological and Medical Laboratory Sciences, Graduate School of Medicine, Nagoya University, Nagoya, Aichi 464-8601, Japan*

[b] *Department of Energy Engineering, Graduate School of Engineering, Nagoya University, Nagoya, Aichi 464-8601, Japan*

[c] *New Industry Creation Hatchery Center (NICHe), Tohoku University, Sendai, Miyagi 980-8578, Japan*

E-mail: s-yama@met.nagoya-u.ac.jp

ABSTRACT: Tritium (H-3) is a pure beta-emitting radionuclide and beta particles have extremely low energy (maximum energy: 18.6 keV). Thus the in-vivo imaging of H-3 is thought to be impossible. However, beta particles emit bremsstrahlung X-rays in subjects that may be imaged from outside of the subjects. We tried to image the bremsstrahlung X-rays from H-3 water using a newly developed radiation imaging system. The developed imaging system used a pixelated Ce-doped $(Gd, La)_2Si_2O_7$ (LaGPS) scintillator plate optically coupled to a flat-panel position-sensitive photomultiplier tube (FP-PMT). Using the imaging system, we conducted bremsstrahlung X-ray imaging from H-3 water in a plastic bag with 37-MBq radioactivity. We obtained tungsten slit mask images with a spatial resolution of ~3 mm full width at half maximum (FWHM). The energy spectrum of the bremsstrahlung X-rays from the H-3 water showed a broad distribution with an average energy of ~10 keV. The measured sensitivities of the LaGPS imaging system for bremsstrahlung X-rays from H-3 water in a plastic bag were 1.8×10^{-7}. We conclude that the imaging of bremsstrahlung X-rays from H-3 water was really possible and it has a potential to be a new method for the in-vivo H-3 imaging of small animals, plants, or materials.

KEYWORDS: Gamma camera, SPECT, PET PET/CT, coronary CT angiography (CTA); Gamma detectors (scintillators, CZT, HPGe, HgI etc); Radiation monitoring; Scintillators, scintillation and light emission processes (solid, gas and liquid scintillators)

[1] Corresponding author.

https://doi.org/10.1088/1748-0221/15/04/P04006

2020 JINST 15 P04006

Contents

1 Introduction

Tritium (H-3) is a beta particle-emitting radionuclide used in the tracer studies of sliced small animals [1, 2] as well as often used in the cell proliferation studies using H-3 labeled tyrosine. H-3 is also used in nuclear fusion research [3]. H-3 is produced in nuclear power plants and its release from the Fukushima Daiichi Nuclear Power Plant (FDNPP) has been documented as a serious problem [4]. H-3 imaging is generally thought to be difficult and impossible from outside of subjects or containers because it is a pure beta-emitting radionuclide and beta particles have extremely low energy (maximum energy: 18.6 keV). Distribution measurements for H-3 have been conducted with autoradiography by directly contacting the sliced subject onto the detector using a beta particle-sensitive plate detector such as X-ray film or an imaging plate (IP). However, care must be taken with the plate's surface coating because the maximum range of H-3 beta particles is short (6 µm) and beta particles are absorbed by the surface coating materials [5, 6]. H-3 contamination of the imaging plates is also a problem [5, 6]. Although imaging systems using photodetectors combined with scintillators were developed and tested to image beta and alpha particles [7–13], H-3 imaging in a subject or container is thought be impossible because of the short range of H-3 beta particles. If the imaging of H-3 in subjects or containers becomes possible, it would be a great advance for radiation measurement research.

Detecting bremsstrahlung X-rays is one possible method of imaging beta-emitting radionuclide from outside of subjects because X-rays can penetrate the subjects or containers. So far, we successfully imaged bremsstrahlung X-rays outside of a plastic container of carbon-14 (C-14) solution that emitted beta particles (maximum energy: 156 keV) [14] using our developed high-resolution Ce-doped (Gd, La)$_2$Si2O$_7$ (LaGPS) radiation imaging system [15]. However, since the energy of the bremsstrahlung X-rays emitted from H-3 is much lower than those of C-14, it would be a challenge to image the bremsstrahlung X-rays emitted from H-3 water. Although detecting bremsstrahlung X-rays from H-3 has been conducted to determine the depth distribution in the materials using a semiconductor detector [16], it has not been used in the imaging of H-3 water distribution. Here, we show the first images of bremsstrahlung X-rays from H-3 water contained in a plastic bag using our developed scintillation imaging detector.

2 Methods

2.1 LaGPS radiation imaging system

The schematic drawing of the radiation imaging detector used in our experiments is shown in figure 1 (A). We developed a larger field of view (FOV) imaging detector than previously used for bremsstrahlung X-rays from C-14 solution [15]. The developed large FOV imaging detector consisted of a pixelated LaGPS plate and a flat-panel position-sensitive photomultiplier tube (FP-PMT). The size of the LaGPS plate was 35 mm × 35 mm × 1 mm thick. We slotted the LaGPS plate into 0.2 mm × 0.2-mm pixels using a dicing method [17]. The pixelated LaGPS plate had 0.2-mm pixels separated by air gaps with widths of 0.1 mm. The LaGPS plate was optically coupled to a 0.5-mm-thick glass support. The pixelated LaGPS plate was optically coupled to a high quantum efficiency (HQE) flat panel photomultiplier tube (FP-PMT) (H12700, Hamamatsu Photonics, Japan) with silicone rubber (KE-420, Shin-Etsu Silicone). The detector surface was covered by an aluminized Mylar sheet for an optical shield and reflector and contained in a 5-mm-thick tungsten container. Figure 1 (B) shows a photo of the imaging detector. The upper surface of the detector case was also covered by a 40-µm-thick black paper for an additional light shield and to prevent mechanical scratches to the aluminum Mylar sheet.

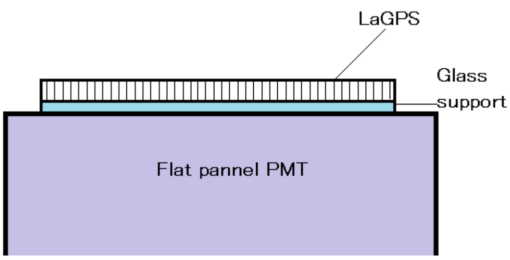

(A)

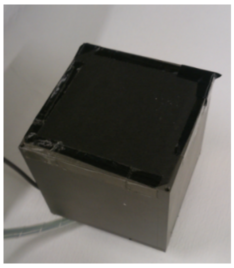

(B)

Figure 1. Schematic drawing of LaGPS imaging detector (A) and photo of the imaging detector contained in tungsten shield (B).

Signals from the FP-PMT were individually amplified and weight-summed by amplifiers to produce four weighted-summed signals. We used the same electronics as previously used for gamma or X-ray cameras [18–20]. We converted the weighted-summed signals to digital signals by four 100-MHz analog-to-digital converters (ADCs). The digitized signals were integrated and used for position calculation based on the Anger principle. The acquired data was sorted into 50 × 50 matrix image with a fixed energy window. The energy window was set from ~5 keV to ~20 keV. For the energy spectrum measurement, we sorted the acquired data into 256 × 256 matrix image

2020 JINST 15 P04006

with energy information. In the acquired image, we set the region of interest (ROI) and derived the energy spectrum for the ROI.

2.2 Imaging experiments of the bremsstrahlung X-rays from H-3 water

In figure 2, we show a schematic drawing of the experimental setup during imaging of the bremsstrahlung X-rays from the H-3 water. One of the tungsten masks shown in figure 3 was set on the imaging detector to absorb the bremsstrahlung X-rays from the H-3 water. We set the H-3 water contained in a plastic bag on the tungsten mask. The plastic bag was 40-μm thick and contained 1 cc of H-3 water with activity of 37 MBq (Moravec Inc., U.S.A.). The thickness of the H-3 water in the plastic bag was ~1 mm. Thus, the beta particles from the H-3 were completely absorbed in the plastic bag while bremsstrahlung X-rays were emitted from the H-3 water. Some of the bremsstrahlung X-rays entered the open space of the tungsten mask and were detected by our LaGPS imaging detector.

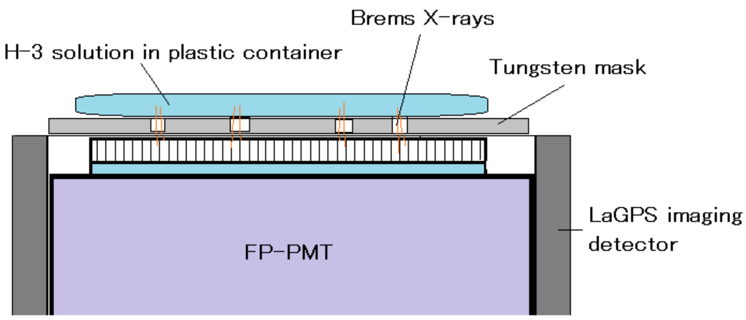

Figure 2. Schematic drawing of imaging experiments of bremsstrahlung X-rays from H-3 water.

We prepared three types of slit masks used for the bremsstrahlung X-ray imaging from H-3 water. One is the square mask shown in figure 3 (A). We used this mask because it appeared easy to observe its shape due to the wider slit separations. The width of the slits was 2 mm and the separation between the slits was 10 mm. We show the tungsten mask used for the evaluation of the spatial resolution in figure 3 (B). This mask had four sectors with silt widths of 1 mm, 1.5 mm, 2 mm, and 2.5 mm. This mask was used for the spatial resolution evaluation of the LaGPS imaging detector for the bremsstrahlung X-rays from H-3 water. We show a character tungsten mask in figure 3 (C). This mask had 2-mm wide slits with the characters "KOBE" in the mask and was used for image quality evaluation. Each imaging was conducted for 660 min. The background image was also measured without the H-3 water source and we subtracted the background image from the measured images.

To evaluate the spatial resolution from the image, we measured an image with a longer time (1200 min) using the spatial resolution mask. We measured the profile on the image and evaluated the spatial resolution.

We also measured the images without masks at different acquisition times to determine image quality. As shown in figure 4, the H-3 water contained in the plastic bag was set on the LaGPS imaging detector surface partially covering the detector's FOV. We conducted imaging at different acquisition times to compare the image quality.

2020 JINST 15 P04006

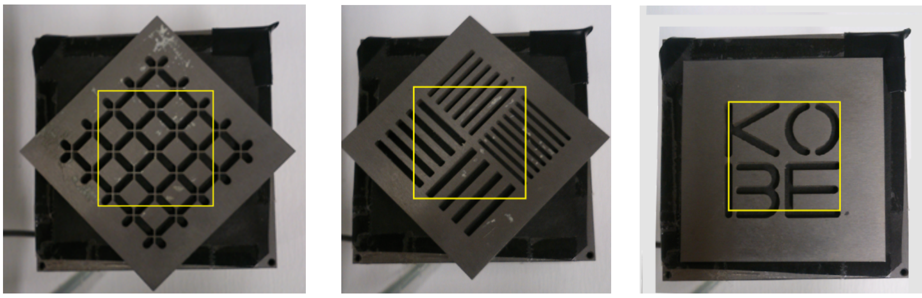

(A) (B) (C)

Figure 3. Slit masks used for imaging experiments: square mask (A), spatial resolution mask (B), and character mask (C). The yellow squares identify the imaging area of the detector.

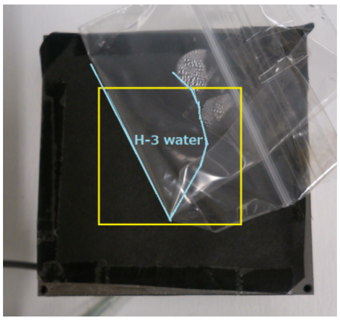

Figure 4. Photo of imaging of H-3 water contained in the plastic bag set on LaGPS imaging detector surface partly covering the detector's FOV. The yellow square is the imaging area of the detector and the blue area shows where the H-3 water is located.

2.3 Energy spectrum and sensitivity measurements of bremsstrahlung X-rays from H-3 water

We measured the energy spectrum without slit masks using the LaGPS imaging detector and derived an energy spectrum for an ROI of the image. From the total counts, we also calculated the sensitivity of the LaGPS imaging detector for the H-3 water contained in the water bag. We defined the sensitivity of the imaging detector for the bremsstrahlung X-rays from H-3 water as count/sec/Bq for 1 mm thick H-3 water contained in a 40-µm thick plastic bag. We compared the energy spectrum and sensitivity with the spectrum calculated by Monte Carlo simulation based on the Geant4 toolkit (version 10.4).

3 Results

3.1 Imaging experiments of bremsstrahlung X-rays from H-3 water

We show the images of the square mask, spatial resolution mask, and character mask by bremsstrahlung X-ray irradiation from the H-3 water in figure 5 (A), (B), and (C), respectively. We can see the square slit shape in figure 5 (A). The spatial resolution phantom in figure 5 (B) shows some of the slits resolved in the images. For the character phantom, we observed some of the "KOBE" characters in the image, as shown in figure 5 (C).

2020 JINST 15 P04006

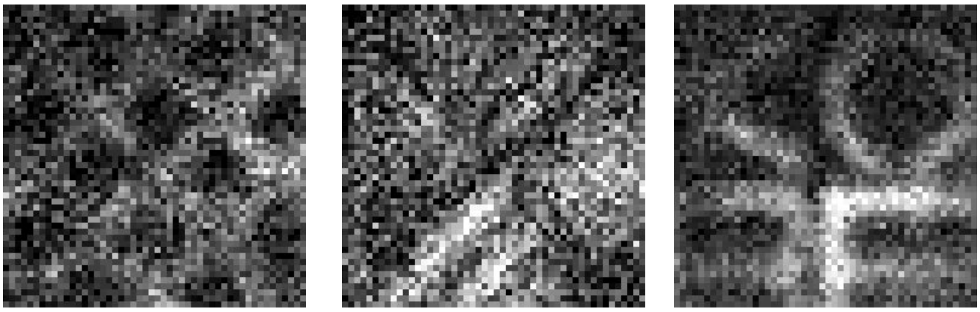

(A) (B) (C)

Figure 5. Images of bremsstrahlung X-rays from H-3 water with slit masks: square mask (A), spatial resolution mask (B), and character mask (C).

Figure 6 (A) shows images of bremsstrahlung X-rays from H-3 water with spatial resolution mask measured for 20 h. The count profile of the yellow line in figure 6 (A) is shown in figure 6 (B). We could observe the peaks with ~3 mm separation (1.5 mm width slits). Since the spatial resolution can be roughly estimated by the double of the width of the slit widths [11], the spatial resolution was estimated to be ~3 mm full width at half maximum (FWHM).

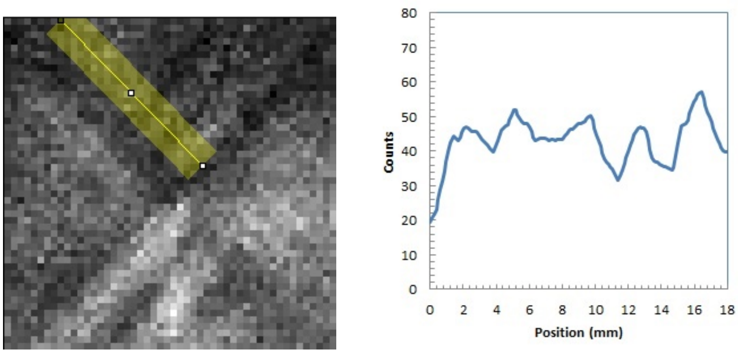

(A) (B)

Figure 6. Images of bremsstrahlung X-rays from H-3 water with spatial resolution mask with 20h acquisition time (A) and count profile (B).

The images without mask at different acquisition times are shown in figure 7 (A) to (C). At an acquisition time of 60 min, we observed distribution of the H-3 water in the image. Even at a 10-min acquisition time, we can see rough distribution of the H-3 water in the image. The nonuniformity of the images was due to the difference in the thickness of the H-3 water in the plastic bag.

We show the energy spectrum of the bremsstrahlung X-rays from the H-3 water in figure 8. The measured energy spectrum in figure 8 was calibrated by the peak of the measured energy spectrum for ~35 keV X-rays from Cs-137. The energy spectrum had a broad distribution of bremsstrahlung X-rays from the H-3 water where their average energy was ~10 keV. The energy spectrum by Monte Carlo simulation is also shown in figure 8, in which we observed a similar distribution to the measured energy spectrum. The measured sensitivity of the LaGPS imaging detector for the bremsstrahlung X-rays from the H-3 water was 1.8×10^{-7}. The calculated sensitivity by Monte Carlo simulation was 1.9×10^{-7}.

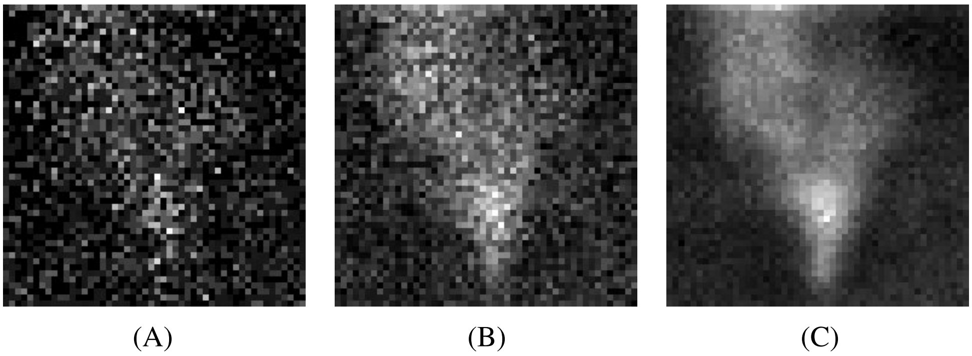

Figure 7. Images of bremsstrahlung X-rays from H-3 water without mask: 10 min (A), 60 min (B), and 660 min (C).

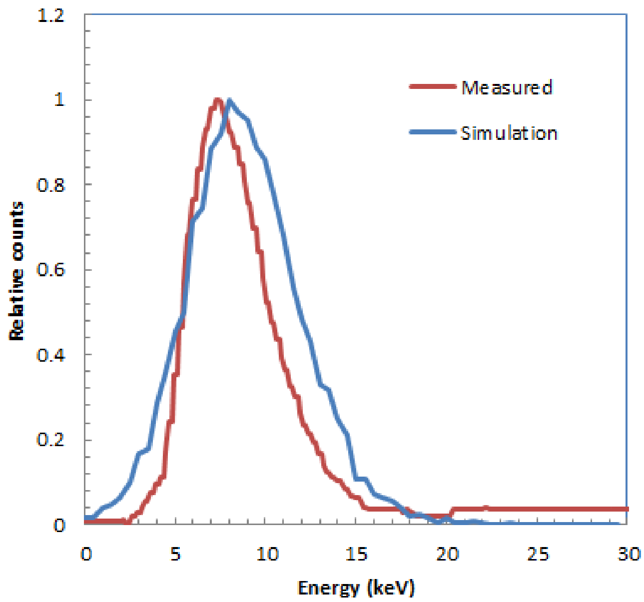

Figure 8. Measured and simulated energy spectra of bremsstrahlung X-rays from H-3 water.

4 Discussion

We successfully imaged the distribution of bremsstrahlung X-rays from H-3 using our LaGPS radiation imaging system. Its intrinsic spatial resolution for bremsstrahlung X-rays from H-3 water was~3 mm FWHM. The spatial resolution for bremsstrahlung X-rays from H-3 water was lower than that for bremsstrahlung X-rays from C-14 solution (1 mm FWHM). The main reason for the low spatial resolution was the low energy of the bremsstrahlung X-rays from H-3, which had 10-keV energy — one third of the average energy of bremsstrahlung X-rays from C-14 solution [14] because the spatial resolution of the Anger principle based camera is roughly determined by the light output of the scintillators [21]. Another reason was that our LaGPS imaging detector had a larger FOV with an FP-PMT with a larger anode size (6 mm × 6 mm). The LaGPS imaging detector used for the bremsstrahlung X-rays from C-14 solution had a cross-wire anode with 4-mm separations [14].

For the imaging of the tungsten masks, we measured 660 min for each imaging. This long acquisition time was due to the low sensitivity (1.8×10^{-7}) of the LaGPS imaging system for bremsstrahlung X-rays from H-3 water. The reason for this low sensitivity was because the bremsstrahlung X-ray emission rate for the H-3 beta particles was ~10^{-6} to ~10^{-7} [22]. In addition, some low-energy bremsstrahlung X-rays were absorbed in the H-3 water or optical shield of the imaging detector. Since the scintillation signals were small for the low-energy bremsstrahlung X-rays, some of these small signals were discriminated by the lower energy threshold and not used for the imaging. However, it was enough to image the H-3 water with our developed LaGPS imaging system. Higher activity of H-3 water will reduce the acquisition time.

One possible application is to in-vivo imaging of H-3 distribution in small animals. The imaging of shallow areas of the body can be imaged by the imaging detector. Imaging without a collimator may be suitable for this imaging [23] because of the low sensitivity for H-3. Imaging the H-3 distribution in plants is also a candidate because some parts of plants, such as leaves, are thin and it is easier for bremsstrahlung X-rays from H-3 to escape. Distribution measurements of H-3 from the distance by using a pinhole collimator may be possible for high-activity distribution of H-3 because bremsstrahlung X-rays from H-3 are not absorbed by air.

5 Conclusions

We successfully imaged bremsstrahlung X-rays from H-3 water using a LaGPS radiation imaging system. The imaging of bremsstrahlung X-rays from H-3 has the potential to be a new method for in-vivo distribution measurement of subjects.

Acknowledgments

This work was partly supported by JSPS KAKENHI Grant Numbers 18K19909 and 18H03469. The authors thank Drs. T. Fukuchi and J. Kataoka for providing and processing the pixelated LaGPS scintillator plate. The authors also thank Mr. Yoshida for the advices on H-3 imaging methods.

References

[1] K. Abe et al., *In vivo imaging of reactive oxygen species in mouse brain by using [3H]hydromethidine as a potential radical trapping radiotracer*, *J. Cereb. Blood Flow Metab.* **34** (2014) 1907.

[2] N. Takai et al., *Imaging of reactive oxygen species using [3 H]hydromethidine in mice with cisplatin-induced nephrotoxicity*, *EJNMMI Res.* **5** (2015) 116.

[3] R.J. Pearson, O. Comsa, L. Stefan and W.J. Nuttalla, *Romanian tritium for nuclear fusion*, *Fusion Sci. Technol.* **71** (2017) 610.

[4] R. Querfeld et al., *Radionuclides in surface waters around the damaged Fukushima Daiichi NPP one month after the accident: Evidence of significant tritium release into the environment*, *Sci. Total Environ.* **689** (2019) 451.

[5] K. Sugiyama et al., *Tritium distribution on the surface of plasma facing carbon tiles used in JET*, *J. Nucl. Mater.* **313** (2003) 507.

[6] K. Sugiyama et al., *Tritium profile in plasma-facing components following D-D operation*, *J. Nucl. Mater.* **329** (2004) 874.

[7] T. Iida et al., *An alpha-particle imaging system for detecting plutonium contamination*, *Nucl. Instrum. Meth.* **212** (1983) 413.

[8] B.W. Miller et al., *The iQID camera: An ionizing-radiation quantum imaging detector*, *Nucl. Instrum. Meth.* **A 767** (2014) 146.

[9] S. Yamamoto, T. Iida and I. Kanno, *Development of a high-resolution alpha camera*, *Nucl. Instrum. Meth.* **A 392** (1997) 291.

[10] S. Yamamoto and T. Iida, *A position-sensitive alpha detector using a thin plastic scintillator combined with a position-sensitive photomultiplier tube*, *Nucl. Instrum. Meth.* **A 418** (1998) 387.

[11] Y. Morishita et al., *Development of a Si-PM based alpha camera for plutonium detection in nuclear fuel facilities*, *Nucl. Instrum. Meth.* **A 747** (2014) 81.

[12] T. Bäck and L. Jacobsson, *The alpha-camera: A quantitative digital autoradiography technique using a charge-coupled device for ex vivo high-resolution bioimaging of alpha-particles*, *J. Nucl. Med.* **51** (2010) 1616.

[13] T. Iida and Y. Ikebe, *A low-energy beta-particle imaging system for measuring tritium distributions*, *Nucl. Instrum. Meth.* **A 253** (1986) 119.

[14] S. Yamamoto, K. Nakanishi, T. Furukawa and H. Tomita, *Possibility analysis of bremsstrahlung x-ray imaging of C-14 radionuclide using a LaGPS radiation imaging system*, *Biomed. Phys. Eng. Express* **5** (2019) 035024.

[15] S. Yamamoto, K. Kamada, S. Kurosawa and A. Yoshikawa, *Development of a high resolution LaGPS imaging detector with pulse shape discrimination capability of different types of radiations*, *Nucl. Instrum. Meth.* **A 922** (2019) 8.

[16] M. Matsuyama et al., *Nondestructive measurement of surface tritium by β-ray induced X-ray spectrometry (BIXS)*, *J. Nucl. Mater.* **290-293** (2001) 437.

[17] S. Yamamoto et al., *Development of a high resolution gamma camera system using finely grooved GAGG scintillator*, *Nucl. Instrum. Meth.* **A 821** (2016) 28.

[18] K. Ando, M. Yamaguchi, S. Yamamoto, T. Toshito and N. Kawachi, *Development of a low-energy x-ray camera for the imaging of secondary electron bremsstrahlung x-ray emitted during proton irradiation for range estimation*, *Phys. Med. Biol.* **62** (2017) 5006.

[19] M. Yamaguchi et al., *Imaging of monochromatic beams by measuring secondary electron bremsstrahlung for carbon-ion therapy using a pinhole x-ray camera*, *Phys. Med. Biol.* **63** (2018) 045016.

[20] S. Yamamoto M. Yamaguchi, T. Akagi, M. Sasano and N. Kawachi, *Development of a YAP(Ce) camera for the imaging of secondary electron bremsstrahlung x-ray emitted during carbon-ion irradiation toward the use of clinical conditions*, *Phys. Med. Biol.* **64** (2019) 135019.

[21] E. Tanaka, T. Hiramoto and N. Nohara, *Scintillation cameras based on new position arithmetics*, *J. Nucl. Med.* **11** (1970) 542.

[22] S. Fukano, *Calculation of bremsstrahlung energy spectrum induced by beta ray*, *Radioisotopes* **52** (2003) 464.

[23] K.L. Walker, M.S. Judenhofer, S.R. Cherry and G.S. Mitchell, *Un-collimated single-photon imaging system for high-sensitivity small animal and plant imaging*, *Phys. Med. Biol.* **60** (2015) 403.

2020 JINST 15 P04006